

Terahertz quantum cascade lasers with sampled lateral gratings for single mode operation

Dixiang SHAO, Chen YAO, Zhanglong FU, Wenjian WAN, Ziping LI, Juncheng CAO (✉)

Key Laboratory of Terahertz Solid-State Technology, Shanghai Institute of Microsystem and Information Technology, Chinese Academy of Sciences, Shanghai 200050, China

© Higher Education Press 2020

Abstract In this paper, we presented single mode terahertz quantum cascade lasers (THz QCLs) with sampled lateral grating emitting approximately 3.4 THz. Due to strong mode selection, the implementation of sampled lateral grating on THz QCL ridges can result in stable single longitudinal mode emission with a side-mode suppression ratio larger than 20 dB. The measured peak power of the grating laser is improved by about 11.8% compared to the power of devices with uniform distributed feedback gratings. Furthermore, the far-field pattern of the presented device is uninfluenced by grating structures.

Keywords terahertz (THz), quantum cascade laser (QCL), sampled lateral grating

1 Introduction

Since the first demonstration in 2002, electrically-pumped, compact, semiconductor terahertz quantum cascade lasers (THz QCLs) have experienced rapid development in the last decades [1,2]. For most applications, such as absorption spectroscopy, telecommunication, and heterodyne mixing in astronomy, single longitudinal mode THz QCLs with wide tuning ranges are necessary. First-, second-, and third-order distributed feedback (DFB) gratings are commonly adopted and designed for THz QCLs to achieve single mode operation [3–7]. Among various structures of DFB gratings, lateral DFB gratings can be simultaneously fabricated with ridge waveguides, so that no extra steps are needed for the conventional fabrication process. THz QCLs with first-order lateral DFB gratings have already been demonstrated for semi-insulating surface-plasmon waveguides with single mode

emission [5]. As an alternative to DFB gratings, the coupled-cavity technique was recently implemented with success in obtaining stable single mode operation for THz QCLs with a side-mode suppression ratio in the 30–40 dB range [8]. On the other hand, THz QCLs with high output power are desirable in most practical applications due to the significant attenuation of THz radiation by water vapor in the atmosphere, which can sometimes decrease the total output power.

In this work, sampled lateral grating, which is expansively used in lasers operating in telecom and mid-infrared wavelengths [9–12], is used to improve output power and obtain single mode operation for THz QCLs. DFB gratings are periodically blanked in the sampled lateral grating, so the optical loss during light propagation caused by the sudden change of waveguide widths of lateral DFB gratings has been reduced when compared with that of DFB lasers with the same device length. Sampled lateral grating can improve the mode selection of lasers, leading to single longitudinal mode operation of devices. In this work, output peak power was improved by about 11.8% compared with that of DFB THz QCLs. The side-mode suppression ratio (SMSR) of the proposed device is larger than 20 dB at 10 K. Sampled lateral grating implementation does not deteriorate the far-field distribution of the present device. Furthermore, due to the adoption of lateral gratings structures, the proposed device has improved simplicity compared to previous models.

2 Design and fabrication

The active region of THz QCLs is based on a bound-to-continuum transition with a one-well injector reported in Ref. [9] (total thickness ~ 11 μm). The designed center frequency of the laser is ~ 3.4 THz. The presented device is processed into a semi-insulating surface-plasmon waveguide structure. The optical mode is confined between the

top metal and the highly n-doped layer below the active region. Fabry-Perot (F-P) lasers based on this type of waveguide typically show higher output power and better beam quality when compared to those based on metal-metal waveguides [13].

The THz QCL structure with sampled lateral grating is depicted in Fig. 1(a), where Λ is the Bragg grating period, Z is the sampling period, Z_g is the length of Bragg gratings in one sampling period, and W_N and W_W are widths of narrow and wide ridges of gratings, respectively. The duty cycle of the sampled grating, d , is defined as Z_g/Z , and the duty cycle of the DFB grating is 0.5. To achieve single lobe far-field patterns, W_W and W_N were chosen to be 120 and 100 μm , respectively, according to finite element simulation. The corresponding calculated fundamental mode profile is shown in Fig. 1(b). The effective refractive indices (n_{eff}) of these two types of waveguides are calculated to be 3.594 and 3.59, respectively. Therefore, the average wavelength λ in the material was calculated to be about 24.56 μm . For first-order gratings, the grating period Λ is 12.28 μm ($\Lambda \sim \lambda/2$), and each sampling period contains 15 DFB periods. Devices with $d = 1$ (corresponding to the uniform DFB grating), $1/2$, and $1/3$ were fabricated for comparison. The mode spacing of sampled lateral grating THz QCLs can be calculated by $\Delta\lambda = \lambda_B^2/(2n_{\text{eff}}Z)$ [14], where λ_B is the Bragg wavelength of the grating. Thus $\Delta\lambda$ are about 2.94 and 1.96 μm for devices with $d = 1/2$ and $1/3$, respectively, which are much larger than that of the F-P laser ($\sim 0.43 \mu\text{m}$ by $\Delta\lambda = \lambda^2/(2n_{\text{eff}}L)$). Therefore, the adoption of sampled lateral grating is helpful for THz QCLs to operate in single longitudinal mode.

Following the growth of the sample by molecular beam epitaxy, Ti-Au metal contacts were evaporated on top of the active region by the E-beam evaporation and lift-off process. To construct the ridged waveguide and sampled lateral grating structures, inductive coupled plasma etching

technology was utilized to etch about 10 μm of the active region. Wet etching was then used to polish the side walls of waveguides and eliminate defects induced by dry etching. The lateral Ge/Au/Ni/Au non-alloy contacts were evaporated and annealed to form the bottom ohmic contacts. After thinning the substrate to about 150 μm , the Ti/Au layers were deposited on the back of the sample. Then samples were cleaved to about 2.5 mm long, soldered onto copper heat sinks with an In/Ag alloy and wire bonded for testing. The final device configuration is shown in Fig. 1(c).

3 Results and discussion

For measurement, devices were mounted on the cold finger of a closed-cycle helium cryostat with a polyethylene window. A Winston cone was used to collect light from the laser facets. Pulsed power-current (P - I) characteristics were measured by a thermopile power meter. Spectra were recorded with a Fourier transform infrared spectrometer (FTIR) in rapid scan mode using a resolution of 0.25 cm^{-1} . Drive current with pulse width of 5 μs at a repetition rate of 5 kHz (duty cycle 1%) was used in all measurements.

Figure 2 shows power-current (P - I) curves of 2.5 mm long sampled lateral grating THz QCLs with $d = 1/3$, $1/2$, and 1 in pulsed mode, respectively. Lasing ceased around 70 K. As shown in Fig. 2, the slope efficiency of the device is 7.32 mW/mA. The threshold current density at 10 K was measured to be about 550 A/cm² for sampled lateral grating THz QCLs, slightly lower than that of DFB THz QCLs (about 600 A/cm²). As clearly shown in Fig. 2(b), the detected maximum peak power of 18 mW measured at 10 K was obtained for sampled lateral grating THz QCLs with $d = 1/3$, while DFB THz QCLs have a maximum peak power of 16.1 mW. The peak power has been improved by about 11.8%, which is primarily attributed to the low optical loss of sampled lateral grating. Devices with $d = 1/2$ have slightly lower output power than that of devices with $d = 1/3$ because more periods of DFB gratings are involved. It can be seen that the peak output power of devices has been increased with the implementation of sampled lateral grating. Although devices with lower duty cycle will have higher output power, the effect of DFB gratings in mode selection will be further weakened, leading to multimode operation in devices multimode operation. A trade-off is necessary between higher output power and stronger ability in mode selection.

Figure 3(a) compares spectra between the F-P laser fabricated on the same wafer and sampled lateral grating THz QCLs with $d = 1/2$ on a logarithmic scale. F-P lasers operate with typical multi-longitudinal modes, while the proposed devices can work in single longitudinal mode by employing sampled lateral grating. Figure 3(b) shows emission spectra of sampled lateral grating THz QCLs with different duty cycles measured at around maximum peak

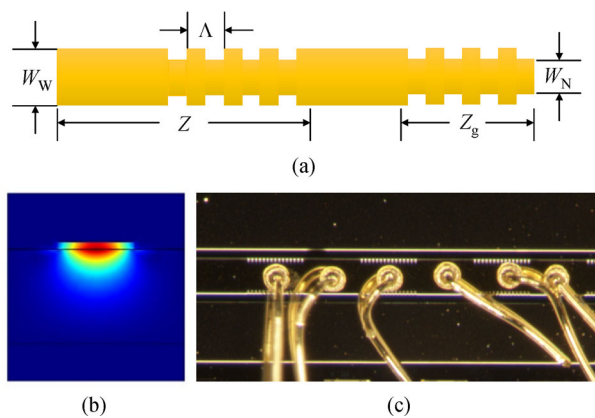


Fig. 1 (a) Schematic diagram of sampled lateral grating THz QCLs. (b) Computed two-dimensional fundamental mode profile of 120 μm -wide waveguide. (c) Top view of the fabricated device

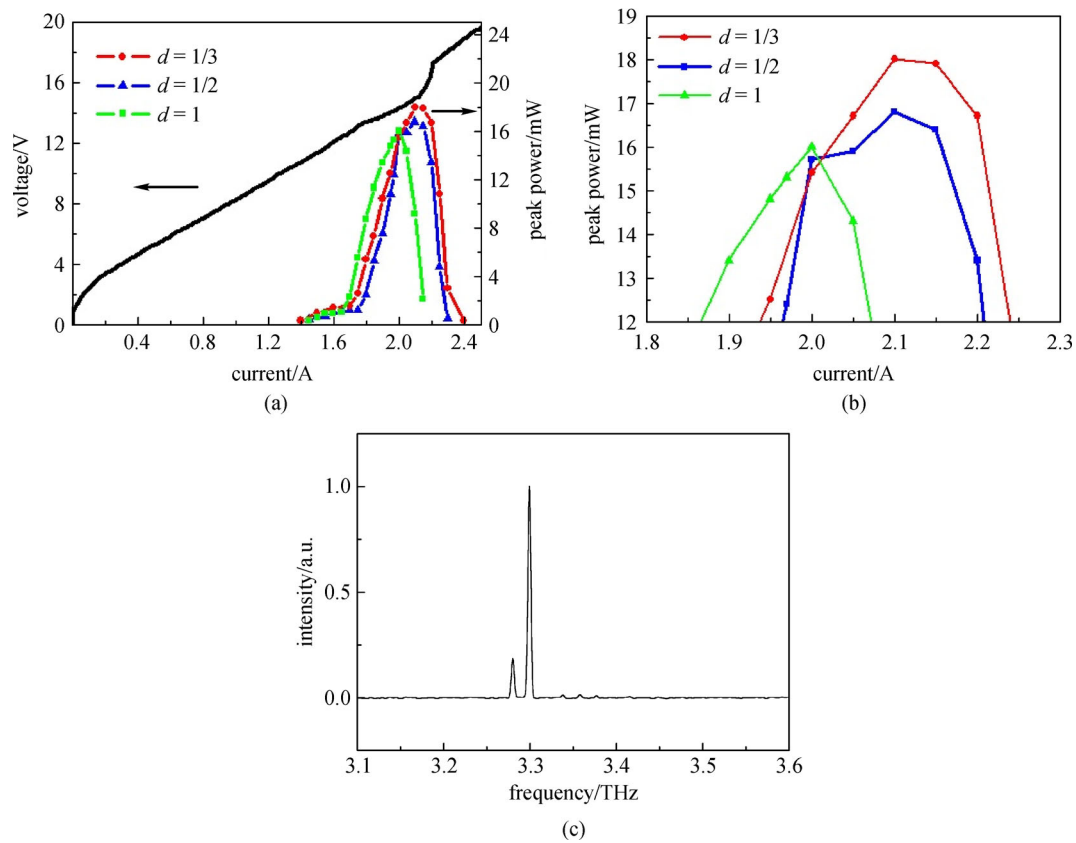


Fig. 2 (a) Power-current (P - I) characteristics of sampled lateral grating THz QCLs measured in pulsed mode at 10 K. Voltage-current characteristics of the device with a grating duty cycle of 1/2 is also shown. (b) Enlarged view of power-current (P - I) characteristics for different sample grating THz QCLs. (c) Emission spectrum of the THz QCL with $d = 1$

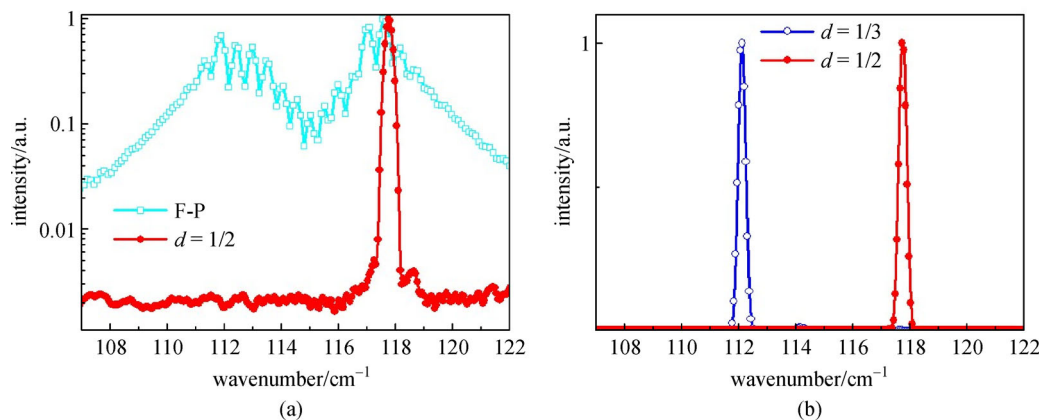


Fig. 3 (a) Emission spectra of sampled lateral grating THz QCLs with $d = 1/2$ and an F-P laser at injection currents near the rollover of power-current (P - I) curves. (b) Emission spectra of sampled lateral grating THz QCLs with $d = 1/3$ and $1/2$ in pulsed mode at injection currents around 2.1 A at 10 K

power. It was observed that emission wavenumbers of these two types of devices were different. This may be due to the influence of the phase difference caused by the position of cleaved facets, leading to the high-frequency or low-frequency DFB lasing modes (both modes are located in the gain spectrum of the laser active region medium)

[14]. SMSRs are ~ 20 dB for devices with $d = 1/3$ and ~ 24 dB for devices with $d = 1/2$, respectively. Under the same device length, devices with $d = 1/3$ have a lower SMSR owing to less sampling periods. Higher SMSR can be achieved when more sampling periods are involved in the devices with longer device length.

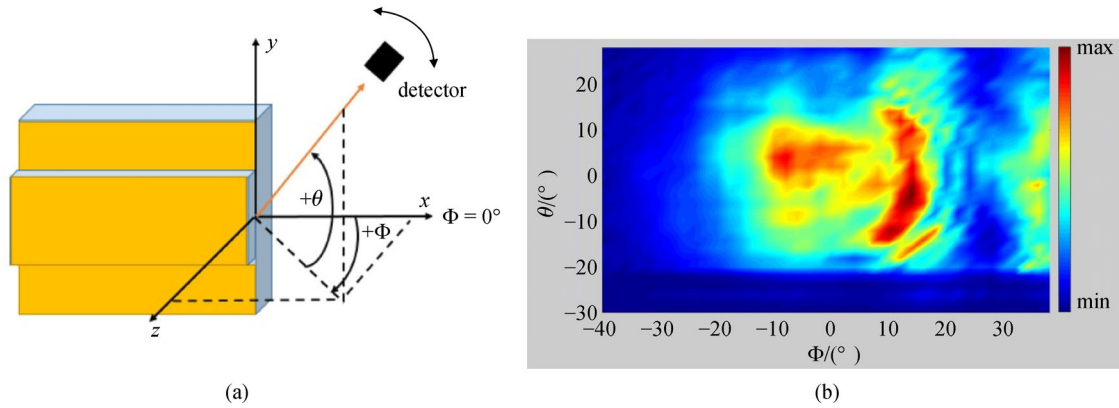


Fig. 4 (a) Schematic diagram of the scanning angles used in far-field measurements. (b) Measured two-dimensional far-field pattern of the sampled lateral grating THz QCL at a drive current of 1.86 A with $d = 1/2$. FWHM is about 44° (θ) \times 40° (Φ)

The far-field patterns of devices were measured by rotating a Golay cell on a spherical surface at constant distance (about 15 cm) from the laser emission facet. Figure 4(b) depicts the typical far-field pattern of sampled lateral grating THz QCLs with $d = 1/2$. Other sampled lateral grating THz QCLs have similar far-field patterns and their results are not shown in this paper. Devices under test operate in single transverse mode as illustrated in Fig. 4(a). A portion of the emitted light was blocked by the cryostat shell when the Golay cell was rotated at a large scanning angle ($\theta < -20^\circ$), which has little influence on far-field intensity pattern measurement. Interference rings appearing in the figure ($\Phi > 20^\circ$) were speculated to be caused by the interference between the radiation from different metallic surfaces of the laser chip or two facets of the laser. The full width at half maximum (FWHM) of the sampled lateral grating THz QCLs was about 44° (θ) in the lateral direction and 40° (Φ) in another direction. Since FWHM of the presented device is similar to that of F-P laser, sampled lateral grating implementation does not deteriorate in the far-field laser distribution.

4 Conclusions

In conclusion, THz QCLs based on sampled lateral grating were proposed and experimentally demonstrated. Using the same length, sampled lateral grating THz QCLs have less gratings area compared with DFB lasers, which causes optical propagation loss due to sudden changes of waveguide width reduction. With the decreased d values, the peak power gradually increases. When $d = 1/3$, the peak power is 18 mW. The output peak power of sampled lateral grating THz QCLs with duty cycle of $1/3$ was improved by about 11.8% compared with that of DFB THz QCLs. The effects of sampled lateral grating in mode selection has been analyzed, and SMSR values larger than 20 dB were obtained. Meanwhile, the adoption of sampled lateral grating has almost no influence on the far-field

device pattern. Furthermore, the presented device can be easily generated by introducing additional fabrication steps, providing an approach to achieve THz sources at low cost, high output power, and single mode operation.

Acknowledgements This work was supported by the National Key R&D Program of China (No. 2018YFB1801502), the National Natural Science Foundation of China (Grant Nos. 61927813, 61975225, and 61704181), the Natural Science Foundation of Shanghai (No. 17ZR1448300), and Shanghai International Cooperation Project (No. 18590780100).

References

1. Kumar S. Recent progress in terahertz quantum cascade lasers. *IEEE Journal of Selected Topics in Quantum Electronics*, 2011, 17(1): 38–47
2. Lin T T, Wang K, Wang L, Hirayama H. High output power THz quantum cascade lasers and their temperature dependent performance. *Journal of Infrared and Millimeter Waves*, 2018, 37(5): 513–518
3. Williams B S, Kumar S, Hu Q, Reno J L. Distributed-feedback terahertz quantum-cascade lasers with laterally corrugated metal waveguides. *Optics Letters*, 2005, 30(21): 2909–2911
4. Mahler L, Tredicucci A, Köhler R, Beltram F, Beere H E, Linfield E H, Ritchie D A. High performance operation of single-mode terahertz quantum cascade lasers with metallic gratings. *Applied Physics Letters*, 2005, 87(18): 181101
5. Wienold M, Tahraoui A, Schrottke L, Sharma R, Lü X, Biermann K, Hey R, Grahn H T. Lateral distributed-feedback gratings for single-mode, high-power terahertz quantum-cascade lasers. *Optics Express*, 2012, 20(10): 11207–11217
6. Amanti M I, Fischer M, Scaliari G, Beck M, Faist J. Low-divergence single-mode terahertz quantum cascade laser. *Nature Photonics*, 2009, 3(10): 586–590
7. Yao C, Xu T H, Wan W J, Li H, Cao J C. Single-mode tapered terahertz quantum cascade lasers with lateral gratings. *Solid-State Electronics*, 2016, 122: 52–55
8. Li H, Manceau J M, Andronico A, Jagtap V, Sirtori C, Li L H,

Linfield E H, Davies A G, Barbieri S. Coupled-cavity terahertz quantum cascade lasers for single mode operation. *Applied Physics Letters*, 2014, 104(24): 241102

9. Lee B G, Belkin M A, Pflugl C, Diehl L, Zhang H A, Audet R M, MacArthur J, Bour D P, Corzine S W, Hofler G E, Capasso F. DFB quantum cascade laser arrays. *IEEE Journal of Quantum Electronics*, 2009, 45(5): 554–565
10. Mansuripur T S, Menzel S, Blanchard R, Diehl L, Pflügl C, Huang Y, Ryou J H, Dupuis R D, Loncar M, Capasso F. Widely tunable mid-infrared quantum cascade lasers using sampled grating reflectors. *Optics Express*, 2012, 20(21): 23339–23348
11. Slivken S, Sengupta S, Razeghi M. High power continuous operation of a widely tunable quantum cascade laser with an integrated amplifier. *Applied Physics Letters*, 2015, 107(25): 251101
12. Jayaraman V, Chuang Z M, Coldren L A. Theory, design, and performance of extended tuning range semiconductor lasers with sampled gratings. *IEEE Journal of Quantum Electronics*, 1993, 29(6): 1824–1834
13. Li L, Chen L, Zhu J, Freeman J, Dean P, Valavanis A, Davies A G, Linfield E H. Terahertz quantum cascade lasers with > 1 W output powers. *Electronics Letters*, 2014, 50(4): 309–311
14. Jayaraman V, Chuang Z M, Coldren L A. Theory, design, and performance of extended tuning range semiconductor lasers with sampled gratings. *IEEE Journal of Quantum Electronics*, 1993, 29(6): 1824–1834



Dixiang Shao received his Bachelor's degree in Electrical Engineering from Southwest Jiaotong University, China in 2013. He received his Ph.D. degree in Optical Engineering from University of Shanghai for Science and Technology, China. His research interest focuses on terahertz optoelectronic devices.



Chen Yao received his Ph.D. degree in Electromagnetic Field and Microwave Technology from Beijing University of Posts and Telecommunications, China. His current research interests include terahertz quantum cascade lasers. He currently works as an engineer at Cisco.



Zhanglong Fu got his Master's degree in Physical Electronics from Xi'an University of Technology, China in 2013. He is currently with Key Laboratory of Terahertz Solid-State Technology, Shanghai Institute of Microsystem and Information Technology, Chinese Academy of Sciences, China. His current research interests include terahertz semiconductor detectors and terahertz imaging.



Wenjian Wan received his Ph.D. degree from University of Chinese Academy of Sciences in 2014. His current research interests include terahertz quantum cascade lasers.



Ziping Li is a postdoctoral researcher at Key Laboratory of Terahertz Solid-State Technology, Shanghai Institute of Microsystem and Information Technology (SIMIT), Chinese Academy of Sciences. He obtained his Ph.D. degree from University of Chinese Academy of Sciences in 2020. Dr. Li's current research interests include terahertz quantum cascade lasers and frequency comb.



Juncheng Cao received his Ph.D. degree in Electrical Engineering from Southeast University, China in 1994. He is currently the Terahertz (THz) group leader and the director of Key Laboratory of Terahertz Solid-State Technology at Shanghai Institute of Microsystem and Information Technology, Chinese Academy of Sciences, China. From 1999 to 2000, he was a Senior Visiting Scientist at National Research Council, Canada. Dr. Cao and his group members successfully developed THz quantum cascade laser and its applications in THz communication and imaging, developed Monte Carlo simulation method for THz quantum cascade lasers, developed THz-radiation-induced semiconductor impact ionized model and successfully explained the absorption of strong THz irradiation in low-dimensional semiconductor. His current research interests include THz semiconductor devices and their applications.